SCALABLE SPARSE SHAPE COMPOSITION AND ITS APPLICATION TO LIVER SURGICAL PLANNING

Guotai Wang[1], Shaoting Zhang[2], Lixu Gu[1]

[1]School of Biomedical Engineering, Shanghai Jiao Tong University, Shanghai, China
[2]Department of Computer Science, University of North Carolina at Charlotte, NC, USA

ABSTRACT

The recently proposed Sparse Shape Composition (SSC) models shape prior as a sparse linear combination of existing shapes. It is effective to represent complex shape variations, with its ability to capture gross errors and preserve local details. However, SSC has low efficiency when dealing with large-scale training data, which adversely affects its more widespread clinical use. In this paper, we investigate efficient and scalable convex optimization methods and propose a nearly real-time SSC for large dataset. The new method solves the convex optimization problem in SSC by continuously transforming it into a series of simplified problems whose solution is fast to compute, without sacrificing the accuracy. It significantly speeds up the shape modeling process. When the repository's capacity is 10000, with 2000 vertices on each shape, the optimization can be solved by the new method in less than 10 seconds, nearly 2000 times faster than traditional method in SSC. Thus, it is more applicable in real-time clinical applications.

Index Terms—Sparse shape composition, shape prior, segmentation, fast optimization, large scale

1. INTRODUCTION

Shape prior based approaches are widely used in medical image segmentation. They are more stable against local image artifacts than traditional methods that solely rely on low-level appearance cues. To obtain patient adaptive shape prior, statistical shape models are usually employed to model shape variations [1, 2], such as the Active Shape Model (ASM), which represents a shape by the mean and variation of a unimodal Gaussian distribution [3]. When shapes follow a multimodal distribution, a mixture of Gaussians may be able to handle them [4]. More general non-linear shape priors may be modeled by manifold learning techniques [5], which overcome the limitation of ASM on statistical constraint. Alternatively, the shape space can be divided into multiple sub-spaces by population-based and patient-specific shape statistics [6, 7].

Sparse Shape Composition (SSC) [8] is a recently proposed method for shape prior modeling. In SSC, a new shape is approximately represented by a sparse combination of shapes in an informative repository. SSC can effectively model complex shape variations, which may be difficult to represent by traditional parametric models. In addition, an input shape may include sparse gross errors, which could be caused by mis-segmentation or erroneous detection. By explicitly modeling gross errors using sparsity constraints, SSC is able to capture them and thus be robust to outliers. Furthermore, SSC can preserve local details even when they are not statistically significant in the repository [8, 9].

SSC has been successfully applied in the liver surgical planning system [9] and other applications. However, its computational efficiency may be limited by the increase of the repository's capacity and the number of vertices on each shape. To obtain efficient shape modeling, one may decrease the repository's capacity or the number of vertices, but the accuracy will also be reduced. Dictionary learning method can improve the speed of computation by reducing the redundancy of the shape repository [10]. However, the dictionary still inevitably loses some important shape information and it needs to be updated every time when new shapes are added to the repository.

In this paper, we introduce a homotopy-based method to quickly solve the convex optimization problem in SSC. Recently, many methods have been proposed in the signal processing and optimization community to solve L1-miminization problems, and the homotopy method shows significantly reduced running time when the signal is very sparse. We adapt this method in the shape prior modeling problem, i.e., to deal with the L1-regulated sparse composition of shapes. The runtime of the new method just increases very slowly when the scale of training samples and the number of vertices grow. This helps SSC maintain high efficiency without lowering accuracy when dealing with large scale training data and shapes with a high number of vertices. Thus, this scalable SSC is more applicable in real-time clinical applications.

2. METHODOLOGY

Sparse Shape Composition: SSC represents shapes by 2D contours or 3D triangular meshes. A shape is denoted as a column vector that is formed by stacking coordinates of all the vertices. A shape containing l vertices with the dimensionality of p can be represented by $d \in R^m$,

where $m = l \times p$. A training repository consisting of n shapes can be denoted as $D = [d_1, d_2, \dots, d_n] \in R^{m \times n}$. All shapes are pre-aligned using generalized Procrustes analysis [3]. Considering an input shape $y \in R^m$, it can be transformed to the common canonical space of D by a spatial transformation operator T with a parameter vector β, i.e., $y' = T(y, \beta)$. The SSC representation is obtained by solving the following L1-norm optimization problem:

$$\min_{x,e}\{\|y' - Dx - e\|_2^2 + \lambda_1(\|x\|_1 + \lambda_2\|e\|_1)\} \qquad (1)$$

where $x \in R^n$ denotes the coefficients for training samples, and $e \in R^m$ represents the gross errors or outliers. λ_1 controls the weight between the L2- and L1-norm, and λ_2 controls the weight between the sparsity of x and that of e.

Linear Programming (LP): The problem in Eq. 1 can be cast as a LP problem

$$\min_{x,w,v}\{\sum_{i=1}^{n} w_i + \lambda_2 \sum_{j=1}^{m} v_j : y' = Dx + e, -w_i \le x_i \le w_i, \\ -v_j \le e_j \le v_j\} \qquad (2)$$

This LP problem can be solved via interior point methods [11], which have a complexity of polynomial time [1]. However, when the problem is large scale, or it involves dense matrix data, the potential advantage of sophisticated interior point methods will often be precluded [12].

Proximal Gradient: x and e can be stacked to form a new vector $x' \in R^{n+m}$, thus the problem in Eq. 1 can be converted to an equal optimization problem that deals with just one variable x'. We define $A = [D\ I(m)] \in R^{m \times (n+m)}$, where $I(m)$ is a unit matrix of size m. Thus, Eq. 1 can be written as:

$$\min_{x'}\{\|y' - Ax'\|_2^2 + \lambda_1\|x'\|_1\} \qquad (3)$$

where the L1-norm is defined as $\|x'\|_1 = \|x\|_1 + \lambda_2\|e\|_1$.

One of the most popular proximal gradient-based algorithms is the iterative shrinkage-thresholding algorithm (ISTA) [13]. The general step of ISTA is:

$$x'_{k+1} = \Phi_{\lambda t}\big(G(x'_k)\big) \qquad (4)$$

where $G(\cdot)$ stands for a gradient step of the fit-to-data least square term in Eq. 3. t is an appropriate step size and Φ_α is a shrinkage operator defined by:

$$\Phi_\alpha(x')_i = (|x'_i| - \alpha)_+ sgn(x'_i) \qquad (5)$$

[1] The current version of released SSC code is based on LP, which is implemented in CVX, a toolbox designed for Disciplined Convex Programs: http://cvxr.com/cvx

The computational cost of ISTA is relatively cheap since each iteration includes matrix-vector multiplication involving A and A^T followed by a shrinkage/soft-threshold step [13]. The advantage of ISTA is its simplicity. However, it has also been recognized as a slow method and it has a worst-case convergence of $O(1/k)$. The fast iterative shrinkage-thresholding algorithm (FISTA) [12] is proposed to accelerate the convergence rate of ISTA. FISTA considers a method that is similar to ISTA. It employs the iterative shrinkage operator at the point which uses a specific linear combination of the previous two points, rather than at the previous point. FISTA preserves the computational simplicity of ISTA but has a global better rate of convergence which is $O(1/k^2)$ [14].

Homotopy Method: The original convex optimization problem in SSC can be continuously transformed into a series of simplified problems whose solution is fast to compute. We consider the following problem:

$$\min_{x'}\{\|y' - Ax'\|_2^2 + \lambda_1\|x'\|_1 + (1-\omega)u^T x'\} \qquad (6)$$

where u is defined as $u = -\lambda_1 z - A^T(A\hat{x} - y')$ and z is a vector that is defined as $sign(\hat{x})$ on the support set of a given warm-start vector $\hat{x}$. ω is a factor ranging from 0 to 1. When $\omega = 0$, the optimal solution for Eq. 6 is $\hat{x}$; as ω changes from 0 to 1, the problem of Eq. 6 will gradually deform to the original one of Eq. 3. At any value of ω, the optimal solution x^* is completely determined by the support set Γ and its sign sequence [15]. Γ changes only at certain nodes of ω [16, 17]. When Γ has not been changed, the direction in which x^* moves is:

$$\partial x' = \begin{cases} (A_\Gamma^T A_\Gamma)^{-1} u_\Gamma, & on\ \Gamma \\ 0, & otherwise \end{cases} \qquad (7)$$

x^* can be moved in direction $\partial x'$ until either one of the optimization constraints [15] is violated, indicating an element should be added to Γ, or one of the nonzero element in x^* shrinks to zero, indicating one element should be removed from Γ. We use δ^* to denote the smallest step-size that leads to one of these changes in Γ. When ω is increased by δ^*, the new optimal solution will become $x^* + \delta^* \partial x'$, and we need to update a Cholesky factorization of $(A_\Gamma^T A_\Gamma)^{-1}$ and $\partial x'$, which has a computational cost of $ms + 3s^2$ flops (assuming there are s elements in Γ). Thus the computational cost of one step is close to the cost of one application of each A and A^T, which is close to $m(n+m) + ms + 3s^2 + O(n+m)$ flops. Thus it is obviously far more effective than LP. In addition, when the warm-start solution $\hat{x}$ is set as 0, the number of steps that $\hat{x}$ will take to deform to the solution of Eq. 3 is approximately determined by the sparsity of the solution. Thus, the homotopy method significantly boosts the computational efficiency compared with the traditional SSC that uses LP, and it also converges much faster than FISTA.

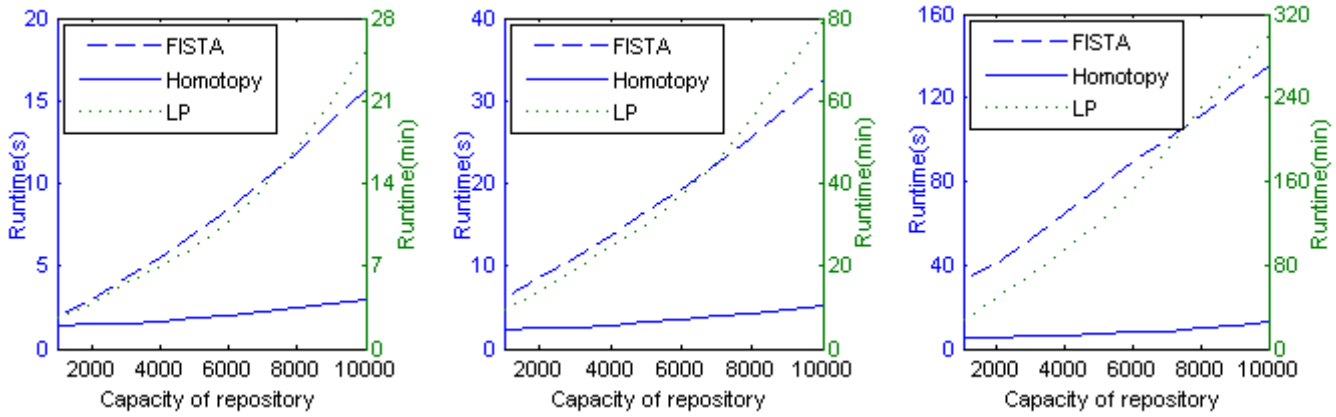

(a) number of vertices:500 (b) number of vertices:1000 (c) number of vertices:2000

Fig. 1. Runtime of SSC with the increase of repository's capacity and number of vertices. FISTA, Homotopy and LP converge to the same accuracy. Please note that the running time of LP is in minute, as shown in the green axis on right.

3. EXPERIMENTS

Experimental Setting: Our algorithm was validated in the application of a liver surgical planning system. SSC was used to model the shape prior of the liver. In the experiments, we focused on the comparison of computational cost of LP, FISTA and homotopy method when they converge to the same accuracy. The repository's capacity was set from 1000 to 10000, and the number of vertices on each shape varied from 500 to 2000. The adaptive focus deformable model (AFDM) [18] was used to obtain one-to-one correspondence of vertices on different meshes. The input liver shape was obtained by a rough liver segmentation based on simple region growing method, which was rapidly performed. The segmentation result was then converted to a surface and registered to the reference shape in the repository. All the experiments were performed on a 3.0 GHz Workstation with 4 cores and 16G RAM, and the algorithms are in MATLAB implementation.

Evaluation of the Computational Efficiency: The average runtimes for the three algorithms are shown in Fig. 1. The results were based on the average performance on 20 cases for each algorithm. Firstly, we tested the performance of these algorithms when the number of vertices was fixed and the repository's capacity changed. In Fig. 1(a), the number of vertices was set as 500. It is shown that with the increase of the repository's capacity, the time consumed by FISTA and LP rose rapidly. In contrast, the homotopy method had a relatively slow increase of runtime with the rise of repository's capacity. When the repository's capacity increased from 1000 to 10000, homotopy method had a runtime ranging from 1.35s to 2.95s, but the time consumed by FISTA increased from 1.97s to 15.75s, and LP consumed 2.56min to 25.33min. Fig. 1(b) and Fig. 1(c) show some similar conclusions.

Fig. 1(a) to Fig. 1(c) show that the runtime of all these algorithms increased when the number of vertices became greater. However, FISTA and LP had an obvious sharp rise of runtime with the increase of vertices number, while the runtime of homotopy method increased very slowly. When the repository's capacity was enlarged to 10000, and the number of vertices was set as 2000, the new method just cost 9.95s, while FISTA and LP cost about 15 times and 2000 times, respectively, of the running time consumed by homotopy method.

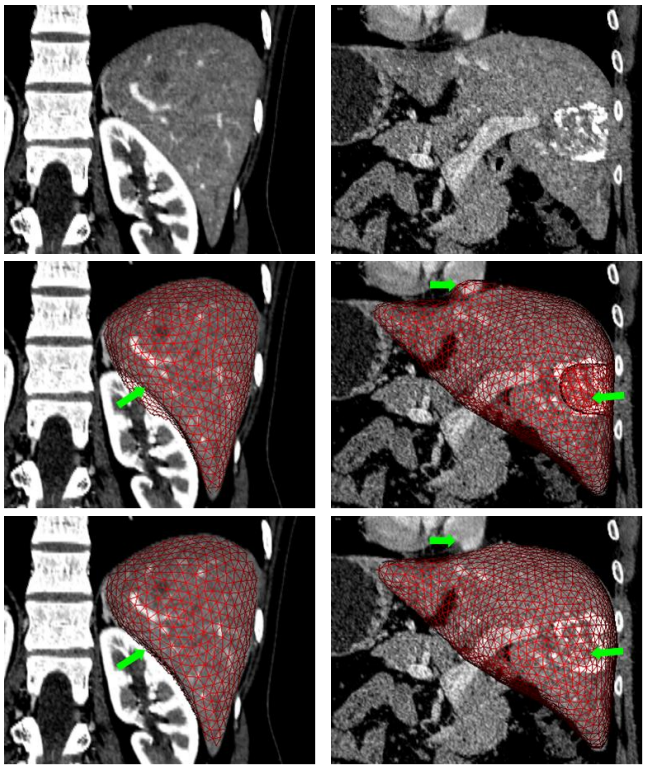

Fig. 2. 3D visualization of SSC shape model. First row: original liver image. Second row: input shape. Third row: result of SSC.

Evaluation of Shape Prior Efficacy: Fig. 2 shows the result of liver shape prior modeling based on the fast SSC. Both the repository's capacity and the number of vertices were set as 2000. In the first column, the kidney led to an over-segmentation, but the SSC excluded the kidney region effectively. In the second column, the patient had a radiofrequency ablation in the past. The gray level of tumor region was obviously different from that of normal regions. The tumor region was not included in the initial segmentation result, and the input shape had a concave region in the right lobe of the liver. The SSC preserved the tumor region in the output shape. In addition, one part of the heart was over-segmented in the input shape, but it was excluded by SSC in the output shape. Furthermore, local details of the input shape, such as corners of the liver, were preserved well in the output shape. We compared the SSC output with manually segmented results. The average symmetric surface distance (ASD) for the two cases in Fig. 2 were 1.28mm and 1.32mm respectively.

4. CONCLUSION

In this paper, we introduced a homotopy method to speed up the convex optimization process in SSC. This method continuously transforms the optimization problem into a series of simplified problems whose solution is fast to compute. Its runtime increases very slowly with the rise of the scale of training data and number of vertices. In conditions where the repository's capacity is very large and the number of vertices is very high, the new method shows a great advantage to quickly solve the optimization problem. Experiments show that SSC is an effective method to model the complex liver shape variations in liver surgical planning system. When the computational efficiency is boosted, SSC becomes more promising to be smoothly applied in clinical environments, with its fast speed and high accuracy. It should be noticed that the new optimization method is general and it can benefit other applications as well.

5. AKNOWLEGEMENT

This research is partially supported by the Chinese NSFC research fund (61190120, 61190124 and 61271318) and biomedical engineering fund of Shanghai Jiao Tong University (YG2012ZD06).

6. REFERENCES

[1] T. Heimann and H.-P. Meinzer, "Statistical shape models for 3D medical image segmentation: A review," *MedIA,* vol. 13, pp. 543-563, 2009.

[2] M. Rousson and N. Paragios, "Shape priors for level set representations," in *ECCV*, pp. 78-92, 2002.

[3] T. F. Cootes, C. J. Taylor, D. H. Cooper, and J. Graham, "Active shape models-their training and application," *CVIU,* vol. 61, pp. 38-59, 1995.

[4] T. F. Cootes and C. J. Taylor, "A mixture model for representing shape variation," *IVC,* vol. 17, pp. 567-573, 1999.

[5] P. Etyngier, F. Segonne, and R. Keriven, "Shape priors using manifold learning techniques," in *ICCV*, pp. 1-8, 2007.

[6] Y. Shi, F. Qi, Z. Xue, L. Chen, K. Ito, H. Matsuo, and D. Shen, "Segmenting lung fields in serial chest radiographs using both population-based and patient-specific shape statistics," *TMI,* vol. 27, pp. 481-494, 2008.

[7] Y. Zhu, X. Papademetris, A. J. Sinusas, and J. S. Duncan, "A dynamical shape prior for LV segmentation from RT3D echocardiography," in *MICCAI*, pp. 206-213, 2009.

[8] S. Zhang, Y. Zhan, M. Dewan, J. Huang, D. N. Metaxas, and X. S. Zhou, "Towards robust and effective shape modeling: Sparse shape composition," *MedIA,* vol. 16, pp. 265-277, 2012.

[9] G. Wang, S. Zhang, F. Li, and L. Gu, "A new segmentation framework based on sparse shape composition in liver surgery planning system," *Medical physics,* vol. 40, p. 051913, 2013.

[10] S. Zhang, Y. Zhan, and D. N. Metaxas, "Deformable segmentation via sparse representation and dictionary learning," *MedIA,* vol. 16, pp. 1385-1396, 2012.

[11] A. Ben-Tal and A. S. Nemirovskiĭ, *Lectures on modern convex optimization: analysis, algorithms, and engineering applications*: Siam, 2001.

[12] A. Beck and M. Teboulle, "A fast iterative shrinkage-thresholding algorithm for linear inverse problems," *SIAM Journal on Imaging Sciences,* vol. 2, pp. 183-202, 2009.

[13] I. Daubechies, M. Defrise, and C. De Mol, "An iterative thresholding algorithm for linear inverse problems with a sparsity constraint," *CMAP,* vol. 57, pp. 1413-1457, 2004.

[14] Y. Nesterov, "A method of solving a convex programming problem with convergence rate O (1/k2)," in *SMD*, pp. 372-376, 1983.

[15] M. S. Asif and J. Romberg, "Sparse Recovery of Streaming Signals Using L1-Homotopy," *CoRR,* vol. abs/1306.3331, 2013.

[16] M. R. Osborne, B. Presnell, and B. A. Turlach, "A new approach to variable selection in least squares problems," *IMA journal of numerical analysis,* vol. 20, pp. 389-403, 2000.

[17] A. Y. Yang, S. S. Sastry, A. Ganesh, and Y. Ma, "Fast ℓ 1-minimization algorithms and an application in robust face recognition: A review," in *ICIP*, pp. 1849-1852, 2010.

[18] D. Shen, E. H. Herskovits, and C. Davatzikos, "An adaptive-focus statistical shape model for segmentation and shape modeling of 3-D brain structures," *TMI,* vol. 20, pp. 257-270, 2001.